

Interaction of Non-Newtonian Fluid Dynamics and Turbulence on the Behavior of Pulp Suspension Flows

Juha-Pekka T. Huhtanen, and Reijo J. Karvinen

Tampere University of Technology, Tampere, Finland.

ABSTRACT

This research paper deals with the interaction of non-Newtonian fluid dynamics and turbulence in paper making flows. Applications are involved with highly non-Newtonian wood fiber and paper pulp suspensions in laminar and turbulent flows. The flow is characterized by using the continuum approach. The goal of the study is to examine the possibilities of using non-Newtonian fluid models for simulation of these flows.

INTRODUCTION

The theories of non-Newtonian fluid dynamics and rheology have for decades been successfully applied in polymer processing, but in the papermaking industry it is only now taking its first steps. Attempts have been made to apply non-Newtonian fluid dynamics to laminar flows of paper pulp suspensions^{1, 2, 3}, but hardly at all to turbulent flow^{4, 5, 6}.

In the study, four distinct flow situations are examined. A pipe flow of dilute pulp suspensions ($C < 4\%$), which is an important pulp transport application from one single process to another, and the pressure losses during the transport are directly related to pumping costs. Flow of concentrated pulp suspensions (up to 10%) in a mixing tank is important for all rotational devices used in papermaking (refiners, mixers, pumps, etc.), because it takes into account the centrifugal force component, which, together with friction

forces, determines pressure production of a hydraulic machine. Flow of dilute water-fiber suspensions ($C < 1\%$) in a converging channel is similar to the flow in a paper machine head-box, and the flow conditions there determine the quality of produced paper. Flow of dilute water-fiber suspensions over a backward facing step is present in many unit processes in paper production, especially in the wet end of paper machine, and is an important mixing element for fiber suspension flows, because it is very effective turbulence generator.

BASIC THEORY

Basics of continuum mechanics and the generalized Newtonian fluid models used in numerical simulations in our study are given below. In addition, the turbulence models used in this study are also expressed.

1. Continuum mechanics

For an incompressible fluid, the continuity equation can be written as

$$\nabla \cdot \mathbf{v} = 0. \quad (1)$$

The conservation law of linear momentum can be written in general form as follows:

$$\rho(D\mathbf{v}/Dt) = \nabla \cdot \mathbf{T} + \mathbf{f}, \quad (2)$$

where \mathbf{T} is the total stress tensor, i.e., Cauchy's stress tensor, and \mathbf{f} is the body

force vector. The first term on the left hand side of the equation is the inertial term with the total derivative of the velocity vector:

$$D\mathbf{v}/Dt = \partial\mathbf{v}/\partial t + \mathbf{v} \cdot \nabla\mathbf{v} . \quad (3)$$

The total stress tensor may be divided into spherical and deviatoric components as follows:

$$\mathbf{T} = -p\delta + \underline{\tau} , \quad (4)$$

where δ is the unit tensor and $p = -(\text{tr } \mathbf{T})/3$ the hydrostatic pressure in the matter.

2. Generalized Newtonian fluid models

In this study, we used only generalized Newtonian models. The term generalized Newtonian fluid is used here to describe behavior, which may be shear thinning or shear thickening, depending on the shear index value. Also start-up stress, often called yield stress, behavior can be described by some of these models. Moreover, the constant viscosity fluid model may also be subsumed within this category.

The following fluid models were used here:

Newtonian fluid:

The behavior of a Newtonian fluid may be described with the aid of a rheological model, which connects the "extra-stress" tensor to the rate of deformation tensor. For an incompressible fluid, the relation can be written as

$$\underline{\tau} = 2\mu \mathbf{D} \quad (5)$$

Power-law fluid:

The shear thinning or shear thickening behavior of materials may be described as an exponential relationship between shear rate and shear stress. The simplest and often a very useful relationship is expressed by the Power-law model, which may be written as

$$\underline{\tau} = K(2(\mathbf{D} : \mathbf{D}))^{(n-1)/2} \mathbf{D} , \quad (6)$$

where n is the Power-law index or shear index, and K is the consistency factor.

Bingham plastic fluid:

Some fluids may exhibit solid type behavior at rest, even a solid body, and hence need finite start-up stress, often called yield stress (τ_y), before they yield and start to flow. Such behavior can be described by the Bingham plastic fluid model in its general form of

$$\underline{\tau} = 2(\tau_y/\gamma + \mu_p) \mathbf{D} , \quad \frac{1}{2}(\underline{\tau} : \underline{\tau}) \geq \tau_y^2 , \quad (7)$$

$$\mathbf{D} = \underline{0} , \quad \frac{1}{2}(\underline{\tau} : \underline{\tau}) < \tau_y^2 , \quad (8)$$

where μ_p is the so-called plastic viscosity.

Herschel-Bulkley fluid:

To combine the advantages of the Power-law and the Bingham plastic fluid models, we can use the Herschel-Bulkley equation to describe the rheological behavior of a fluid

$$\underline{\tau} = 2(\tau_y/\gamma + K\gamma^{(n-1)}) \mathbf{D} , \quad \frac{1}{2}(\underline{\tau} : \underline{\tau}) \geq \tau_y^2 , \quad (9)$$

$$\mathbf{D} = \underline{0} , \quad \frac{1}{2}(\underline{\tau} : \underline{\tau}) < \tau_y^2 , \quad (10)$$

The model describes both yield stress behavior and shear thinning or thickening effects.

Bird-Carreau fluid:

Perhaps the most convenient of the generalized Newtonian models is the Bird-Carreau fluid model

$$\underline{\tau} = 2\mu_\infty \mathbf{D} + (\mu_0 - \mu_\infty) \left\{ [1 + 2\lambda_t] \right\}^2 (\mathbf{D} : \mathbf{D})^{(n-1)/2} \quad (11)$$

where μ_0 and μ_∞ are the first and second Newtonian viscosities at zero and infinite shear rates, respectively, and λ_t is the inverse of a cut-off shear rate in the viscosity curve, often called the characteristic time of the fluid or time

constant. (More on rheological models can be found in the literature⁷.)

3. Turbulence

Non-Newtonian fluids are highly viscous fluids with their apparent molecular viscosities exceeding at low shear rates thousands of times the viscosity of water. However, many non-Newtonian fluids are also shear thinning, which means that more and more bonds between molecules or particles in suspension are broken as the shear rate increases and the fluid's apparent molecular viscosity decreases. The flow field's inertial forces may now become greater than the viscous forces and make the flow turbulent.

One way to approach the problem is to combine the two theories, non-Newtonian fluid dynamics and turbulence, by exploiting the effective viscosity, which links the effects of molecular and turbulent viscosities as follows:

$$\mu_{\text{eff}} = \mu_{\text{ap}} + \mu_t, \quad (12)$$

where μ_t is the turbulent dynamic viscosity, defined in terms of the turbulence kinetic energy (k) and dissipation rate (ε)

$$\mu_t = \rho C_\mu k^2 / \varepsilon. \quad (13)$$

When the Reynolds decomposition is inserted in the momentum equations, Eq. (3), the form of the equations remains, if the new denotation is taken for the total stress tensor. Taking into account both the laminar and turbulent contributions of motion, we can now write the new stress tensor for a turbulent flow field in tensorial notation as

$$\mathbf{T} = -p\delta + \underline{\tau} - \rho\mathbf{Q}, \quad (14)$$

where $\mathbf{Q} = \overline{\mathbf{v}'\mathbf{v}'}$ is the velocity fluctuation correlation tensor defined by the velocity fluctuation vector in (\mathbf{v}'). The overhead bar denotes time averaging.

To evaluate the turbulent viscosity for calculation, we need to determine the values of turbulent quantities or turbulence kinetic energy and the dissipation rate. And to do this, we need a turbulence model to describe turbulent flow behavior. In fact, the same equations as defined in previous section, i.e., continuity and momentum equations, determine the transport phenomena in the main flow field. Since we can write similar transport equations for the above turbulent quantities, we can also determine the turbulent viscosity at every single point in the flow field.

Turbulent quantities in the flow field can be characterized in several different ways, and different turbulence models are categorized based on of the number of equations needed to determine the quantities. In engineering applications, the k - ε model is the best known. More enriched models may be categorized under multi-equation models; their ability to describe turbulence quantities depends on the number of additional equations employed. (More on turbulence as phenomenon and its models can be found in the literature⁸.)

k - ε model:

When we use the k - ε model, we exploit two additional scalar transport equations in addition to the continuity and momentum equations for isothermal flow, one for turbulence kinetic energy and one for dissipation rate. Those equations can be written as follows:

$$\rho (Dk/Dt) = \nabla \cdot (\mu_{\text{eff}} \nabla k) + P_k - \rho\varepsilon, \quad (15)$$

$$\rho (D\varepsilon/Dt) = \nabla \cdot ((\mu_{\text{ap}} + (\mu_t/\sigma_\varepsilon)) \nabla \varepsilon) + \varepsilon(C_{1\varepsilon}P_k - \rho C_{2\varepsilon}\varepsilon)/k, \quad (16)$$

where $C_{1\varepsilon} = 1.44$, $C_{2\varepsilon} = 1.92$, and $\sigma_\varepsilon = 1.3$ are constants.

P_k is the turbulence energy production term, which describes how turbulence takes its energy from the main flow field via

viscous dissipation. Since this happens through deformation work in the main flow field, turbulence energy production is determined by the rate of strain tensor (\mathbf{S}), or by the velocity vector gradient as follows

$$P_k = \mu_t \mathbf{S}^2 = \mu_t (\mathbf{D} : \nabla \mathbf{v}) \quad (17)$$

This straining motion of the main flow field produces velocity fluctuations in the velocity field and thereby feeds energy into the turbulent motion. Therefore, the production of turbulence kinetic energy can be defined also by these velocity fluctuations as

$$P_k = -\rho(\mathbf{Q} : \mathbf{S}) \quad (18)$$

The biggest problem with the k- ϵ model is that it assumes turbulence to be homogenous and isotropic and cannot take into account non-isotropic turbulence. If the streamlines are curved, the straining motion of the main flow field stretches also turbulent vortices and thereby dampens velocity fluctuation in the cross flow direction and amplifies fluctuation in the main flow direction. To take this feature into account, we must resort to more enriched models.

Reynolds stress model:

In the Reynolds stress model (RSM), additional transport equations are needed for each velocity fluctuation correlation component of the dyadic product $\mathbf{v}'\mathbf{v}'$ (Reynolds stress component). In full 3-D simulation, this means six new equations, since the Reynolds stress tensor (\mathbf{Q}) is symmetric. With the earlier definition of the velocity fluctuation correlation tensor (\mathbf{Q}), we can write the transport equations for the Reynolds stress components as

$$\begin{aligned} \rho(D\mathbf{Q}/Dt) = & -\nabla \cdot \left\{ \rho \overline{\mathbf{Q}\mathbf{v}'} + \overline{p'[(\mathbf{v}'\underline{\delta}) + (\mathbf{v}'\underline{\delta})^T]} \right\} + \\ & \nabla \cdot [\mu_{\text{eff}} \nabla \mathbf{Q}] - \rho [\mathbf{Q} \cdot (\nabla \mathbf{v})^T + \mathbf{Q}^T \cdot \nabla \mathbf{v}] + \\ & \overline{p'[\nabla \mathbf{v}' + (\nabla \mathbf{v}')^T]} - 2\mu_{\text{eff}} (\nabla \mathbf{v}' \cdot \nabla \mathbf{v}') \quad (19) \end{aligned}$$

where \mathbf{v}' is the velocity fluctuation vector. From the correlation of the velocity fluctuation components, we can determine the turbulence kinetic energy field by

$$k = \frac{1}{2} (\text{tr } \mathbf{Q}) \quad (20)$$

The transport equation for the turbulence dissipation rate is similar to that defined for the k- ϵ model.

EXPERIMENTS

For this study, a representative set of measurements was prepared to characterize the rheological properties of paper pulp and fiber suspensions to view the subject as a whole. Measurements were also extended to the turbulent flow region to observe the above suspensions in this situation. Furthermore, measurements by other researchers were analyzed and their experimental studies consulted, especially when the rheological properties of the pulp suspensions were analyzed.

Mixing tank:

Bleached softwood kraft pulp suspensions of 2-10% consistency, mixed with a rotating disc type mixer in a container, were rheologically measured at the laboratory of the Energy and Process Engineering Institute, TUT. The container was designed so as to prevent the walls from affecting the shear stress on the rotating disc and hence its torque resistance. The equipment was run by an electromotor, mounted on bearings, and torque resistance was measured on its axle.

The shear stress on the edge of the rotating disc may be calculated from the measured torque values⁶, and we can construct either a shear rate-shear stress or a shear rate-apparent viscosity relation to describe the non-Newtonian behavior of paper pulp or fiber suspensions (see Fig.1).

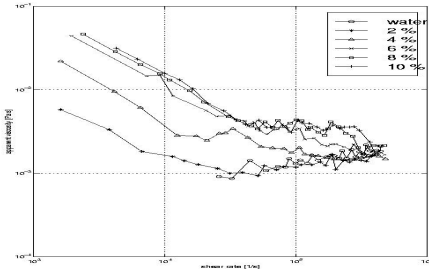


Figure 1. Results of torque measurements with rotating disc in container for water and for bleached softwood kraft pulp suspensions as shear rate-apparent viscosity data.

Pipe flow:

In terms of rheological measurements, pipe flow is very interesting because it is viscometric flow, which can be solved analytically by derivation. The solution can be applied to characterize material properties of fluids with a simple material function such as the Power-law model. If we adopt the notion that pressure drop in pipe flow is equal to the shear stress on the wall, both multiplied by appropriate surface areas, and if we assume that the shear stress of paper pulp or fiber suspensions on the wall can be expressed by the Power-law model, then pressure drop in a laminar case can be written as^{2, 7}

$$dp/dx = -2KV^n(3 + 1/n)^n / R^{(n+1)}, \quad (21)$$

and in a turbulent case⁸

$$dp/dx = 4f\rho V^2 / 2D \quad (22)$$

where the friction factor (f) can be determined by Blasius's type of equation, by using 1/8-law for the velocity profile, as /6/

$$4f = 0.0964 / Re_c^{2/9} \quad (23)$$

Here $Re_c = \rho D^n V^{(2-n)} / (8^{(n-1)} K')$ is the modified Reynolds number, and $K' = K [(3n + 1) / (4n)]^n$ is the modified Power-law consistency.

The measured data used here was adopted from an article by Hämström et al.⁹, which examined the pipe flow of dilute fiber suspensions (0.67%, 1.27%, 2.47% and 3.41%) of bleached softwood kraft pulp. Measurements were made in a 100mm straight pipe by varying the suspension's flow rate. The mean velocity in the pipe was determined from the flow rate and used as reference in pressure drop calculations. These measurements were reanalyzed because of their good documentation and convenience.

Converging channel:

Flow of a non-Newtonian fluid through the converging channel is relevant especially to the paper making industry, because it resembles flow through the slice channel in the paper machine headbox. Such flows are usually turbulent in the core region. However, with viscous fluids some signs of re-laminarization may appear in the boundary layer. To analyze the role of turbulence in the headbox and its effects on produced paper quality, some measurements must be made inside the channel.

In this study, we did not measure flow in a converging channel ourselves but analyzed the measurements by Parsheh et al.¹⁰ to verify our computational results. The measurements were made with air, therefore they are not exactly relevant for fiber suspension flow, but they were the best ones in hands at the moment of this study.

Backward-facing step:

The flow of a non-Newtonian fluid through a channel with a backward-facing step is important in the paper making industry, because the step is often used to create turbulence. In such applications, the flow always separates from the wall and then re-attaches. The separation is necessary to produce turbulence, and highly fluctuating velocities appear in the mixing layer between the main flow stream and the backflow behind the step.

In this study, we did not measure flow in a channel with a backward-facing step but analyzed the measurements by Piirto et al.¹¹ to verify our computations. They used a Particle Image Velocimetry (PIV) in their measurements and aimed to locate the highly turbulent flow areas and to measure their velocity fluctuation components. From the velocity fluctuations, they could calculate the kinetic energy and dissipation rate of the turbulence by using image processing methods.

NUMERICAL SIMULATIONS

All the cases were numerically simulated with commercial codes either in a laminar case with the finite-element-method-based POLYFLOW, versions 3.5.4 to 3.8.0, or in a turbulent case with the control-volume-method-based FLUENT, versions 4.3.2 to 5.5.14. POLYFLOW was chosen for laminar simulations, because experiments showed that paper pulp and fiber suspensions displayed non-Newtonian and viscoelastic properties. FLUENT was used to simulate turbulent flow, because the program can exploit non-Newtonian fluid models for such simulation.

Mixing tank:

We simulated laminar flow of pulp suspensions with POLYFLOW, version 3.5.4, near a rotating disc in a mixing tank, and analyzed and compared the results with the experiments discussed earlier in previous report². In the simulations, we used some generalized Newtonian fluid models (constant viscosity, Power-law, Bingham plastic, Herschel-Bulkley, and Bird-Carreau models). Material functions were determined based on measurements made in our laboratory at TUT.

All the fluid models we used predicted increased torque resistance as a function of the fiber consistency of the paper pulp suspensions, and the increase was almost exponential. However, the Power-law model could not produce accurate torque values, because it cannot take into account complex

non-Newtonian effects, such as yield stress, but only shear thinning. Compared with measurements, those predicted by the Power-law model were more than 100% in error. The Bird-Carreau model, too, failed to predict accurate torque resistances at higher consistencies ($C > 6\%$), the reason possibly being that the model does not actually describe any yield stress effects, but defines explicitly material's zero and infinite viscosity values. Though in terms of numerical simulation, the material models with yield stress behavior (Bingham plastic and Herschel-Bulkley models) were the most difficult to handle, they described physically most accurately the behavior of pulp suspensions in rotational flow. Their predicted results fell within 10-20% of those obtained with measurements for torque resistance. Fig. 2 shows the torque resistances of the disc, calculated based on numerical predictions.

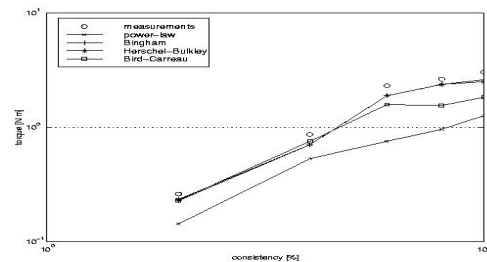


Figure 2. Torque resistance of disc: a) laminar flow ($N = 100$ rpm) with different fluid models as function of fiber consistency.

We simulated turbulent flow of pulp suspensions in a mixing tank with FLUENT, version 5.5.14. We used Power-law fluid model, with the same material parameters as in the laminar series, because the model was presently the only non-Newtonian fluid model available in FLUENT to simulate turbulent flow. Both the k-e and RSM turbulence models were tested in simulation with two different boundary treatment schemes, standard wall functions and two-layer zones, respectively. Fig. 3 shows the disc's torque resistances in turbulent water flow with different turbulence models.

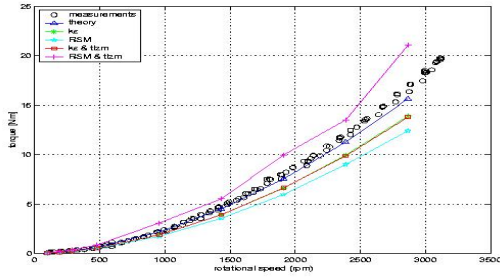


Figure 3. Torque resistance of disc: turbulent flow of water as function of rotational speed of disc, calculated based on numerical predictions and compared with measured data.

Pipe flow:

Laminar paper pulp suspension flow in a pipe was numerically simulated with POLYFLOW, by constructing a 2-D computational domain of a pipe cross-section, through which a volumetric flow rate was imposed. A slip friction boundary condition was introduced on the pipe wall, and slip factor values were determined by analyzing² the measurements of Hemström et al.⁹.

When the measurements were analyzed, the same trend was observed in each case: slip factor values seemed to exhibit a kind of power-law relation with fluid velocity. The results of simulated pressure loss curves with slip boundary condition are shown in Fig. 4.

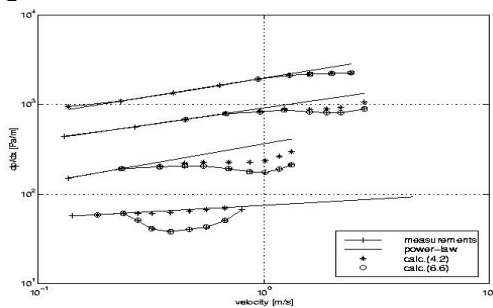


Figure 4. Results of simulated pressure loss in paper pulp suspension flow in pipe².

In this study, we did not simulate numerically turbulent flow in a pipe but compared measurements with theoretical calculations in equations, where the pressure

loss was determined by using the Power-law fluid model as a material function to define the friction factor of pulp suspension in pipe flow. The calculations fully agreed with the measurements. By using the 1/8-law for the velocity profile instead of the normal 1/7-law for Newtonian fluids to determine the friction factor for turbulent pipe flow of non-Newtonian fluid, we could predict the pressure loss very well. Measured and calculated results are compared in Fig. 5.

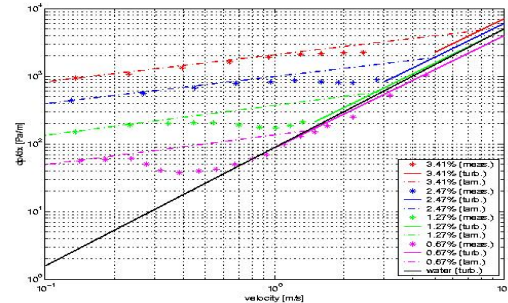


Figure 5. Comparison of measured and calculated pressure losses in pulp suspensions in turbulent pipe flow.

Converging channel:

In numerical simulation of converging channel flow with FLUENT, version 5.3, we used the non-Newtonian Power-law fluid model as a material function and studied in series the effects on turbulence quantities of non-constant molecular viscosity and level of viscosity. The objective was to study the effects of shear thinning by varying the exponent (n) value rather than to try to correctly model fiber suspension as non-Newtonian material. The effects were significant.

Signs of re-laminarization near the walls in the boundary layer can be seen in the velocity profiles in Fig. 6 for water and certain non-Newtonian fluids as a function of the shear index. The consistency of the Power-law model ($K = 100 \cdot \mu_v$) was kept constant throughout the simulations, which gave us the variation of acceleration parameter¹⁰ from $4.89 \cdot 10^{-7}$ to $4.89 \cdot 10^{-5}$, which should indicate the evident change from turbulent to laminar boundary layer.

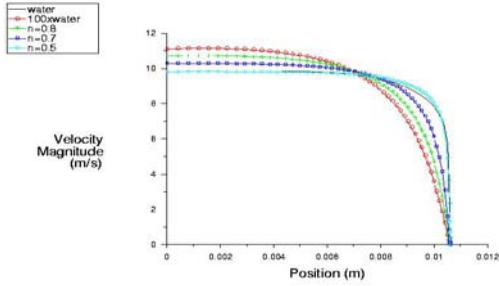


Figure 6. Effect of shear index on velocity profiles in converging channel flow. Simulations of water and Power-law fluids with $K = 100 * \mu_v$.

In a flow domain where the cross section is not constant, as in a contracting channel, turbulence is non-isotropic. In such a case, the RSM turbulence model must be used in order to describe correctly the effects on turbulence quantities of the main strain rate field through eddy stretching. The level of velocity fluctuation in the flow direction is almost an order of magnitude higher than in the cross direction at the end of the channel. The results of the velocity and turbulence quantity profiles agree qualitatively with the measurements by Parsheh et al.¹⁰.

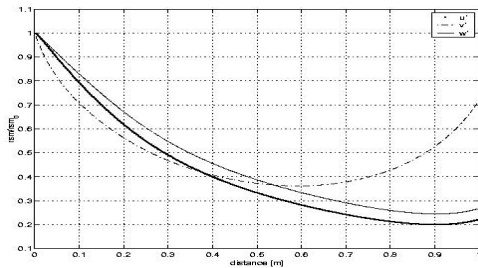


Figure 7. Development of scaled rms values of velocity fluctuations (u' , v' and w') along channel axis for water flow.

Backward-facing step:

We simulated flow over the backward-facing step numerically with FLUENT, version 5.3, and used both the $k-\epsilon$ and RSM turbulence models with standard wall functions or a two-layer wall to compare the accuracy of the two schemes in the wall layer. The Power-law model was used to simulate the shear-thinning behavior of the material.

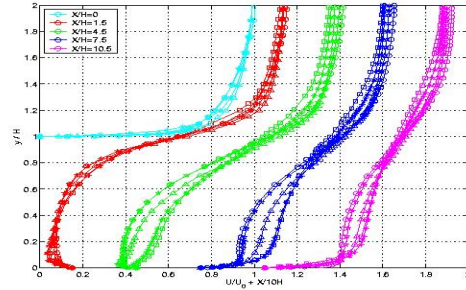


Figure 8. Effects of shear index and consistency values [$(\square) \mu = \mu_v$, $(o) \mu = 10 * \mu_v$, $(*) K = 10 * \mu_v$ & $n = 0.8$, $(\Delta) K = 10 * \mu_v$ & $n = 0.7$, $(+)$ $K = 10 * \mu_v$ & $n = 0.5$] on velocity profile in channel flow after backward facing step.

Our simulations agreed quite well with earlier measurements¹², and simulations¹³. The dimensionless mean flow and turbulence quantity profiles, predicted by different turbulence models, agreed, in fact, excellently with earlier DNS simulations by Le et al.¹³. This is encouraging, because Le et al. analyzed a great number of well-established measurements. However, comparison with measurements made at TUT by Piirto et al.¹¹ indicated some differences, especially in the core flow area. Measurements by Piirto et al. showed too flat velocity profiles and hence too low velocity fluctuation and turbulence kinetic energy. Yet our prediction of the trends coincided with the trends of their measurement, even when fibers were added to the flow.

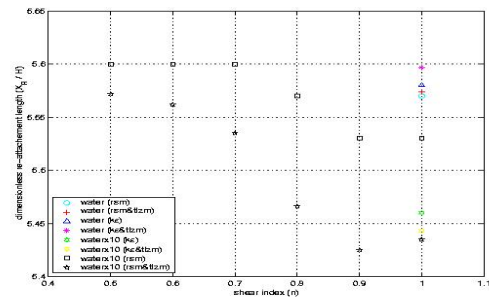


Figure 9. Effect of shear index on location of re-attachment point (X_R / H) after backward-facing step.

The shear index had a marked effect on the location of the re-attachment point after the backward-facing step. As the index decreased, so did also the local molecular viscosity near the walls, and the location of the re-attachment point moved further downstream, as shown in Fig. 9 above.

DISCUSSION AND CONCLUSIONS

This study examined the behavior of paper pulp and wood fiber suspension flows in the paper making industry with focus on continuum mechanics and turbulence. Both the above materials are concentrated suspensions, and therefore their response to a shear stress or shear rate field was analyzed in terms of rheology.

Continuum mechanics and non-Newtonian fluid dynamics combined with turbulence theory turned out to be a suitable theoretical framework to simulate flows in the paper making processes. Though we have to keep in mind the limitations of continuum models, numerical simulation does offer obvious advantages in flow conditions such as these, where accurate measurements are tedious and time-consuming and sometimes even impossible. Simulation of concentrated suspensions in turbulent flow is practically impossible by means other than homogenous models, such as non-Newtonian fluid models. But together with proper turbulence models and wall treatment schemes, these fluid models yield quite reliable results compared to flow measurements. Therefore, the combinatory approach of non-Newtonian fluid dynamics and turbulence theories can be considered successful and one of the most interesting future fields of modern flow simulation.

REFERENCES

1. Wikström, T. (1998), Flow of Pulp Suspensions at Low Shear Rates. Licentiate Thesis, Chalmers University of Technology, Department of Chemical Engineering Design.
2. Huhtanen, J-P. (1998), Non-Newtonian Flows in Paper Making. Licentiate Thesis, Tampere University of Technology, Energy and Process Engineering.
3. Swerin, A. (1995), Flocculation and fiber network strength in papermaking suspensions flocculated by retention aid systems. Doctoral Thesis, Royal Institute of Technology, Department of Pulp and Paper Chemistry and Technology, Division of Paper Technology, Stockholm.
4. Wikstömin, T. (2002), Flow and Rheology of Pulp Suspensions at Medium Consistency. Doctoral Thesis, Chalmers University of Technology, Department of Chemical Engineering Design.
5. Hammarström, D. (2004), A Model for Simulation of Fiber Suspension Flows. Licentiate thesis, Technical Reports from KTH Mechanics, Royal Institute of Technology, Stockholm, Sweden.
6. Huhtanen, J-P. (2004), Modeling of Fiber Suspension Flows in Refiner and Other Papermaking Processes by Combining Non-Newtonian Fluid Dynamics and Turbulence. Doctoral Thesis, Tampere University of Technology, Energy and Process Engineering.
7. Tanner, R. I. (1985), Engineering Rheology. The Oxford Engineering Science Series. Clarendon Press, Oxford.
8. Tennekes, H., Lumley, J. L. (1972), A First Course in Turbulence. MIT Press, Cambridge, Massachusetts.
9. Hemström, G., Möller, K., Norman, B. (1976), Boundary Layer Studies in Pulp Suspension Flow. *TAPPI Journal*, **59**, 115-118.

10. Parsheh, M. (2001), Flow in Contractions with Application to Headbox. Doctoral Thesis, Royal Institute of Technology, Stockholm.
11. Piirto, M. (2003), Characterization and Control of Turbulence with Particle Image Velocimetry in a Backward-Facing Step Flow. Doctoral Thesis, Tampere University of Technology, Energy and Process Engineering.
12. Jovic, S., Driver, D. M. (1994), Backward-facing step measurement at low Reynolds number, $Re_h = 5000$. *NASA Tech. Mem.* 108807.
13. Le, H., Moin, P., Kim, J. (1997), Direct Numerical Simulation of Turbulent Flow Over Backward-facing Step. *J. Fluid Mech.*, **330**, 349-374.